ARTHRITIS & RHEUMATOLOGY
Vol. 66, No. 12, December 2014, pp 3359–3370
DOI 10.1002/art.38888

Vimentin Is a Dominant Target of In Situ Humoral Immunity in Human Lupus Tubulointerstitial Nephritis

Andrew J. Kinloch,[1] Anthony Chang,[2] Kichul Ko,[1] Carole J. Henry Dunand,[1] Scott Henderson,[1] Mark Maienschein-Cline,[3] Natalya Kaverina,[1] Brad H. Rovin,[4] Marlene Salgado Ferrer,[1] Don Wolfgeher,[1] Vladimir Liarski,[1] D. James Haddon,[5] Paul J. Utz,[5] Patrick C. Wilson,[1] and Marcus R. Clark[1]

Objective. **In lupus nephritis (LN), severe tubulointerstitial inflammation (TII) predicts progression to renal failure. Severe TII is associated with tertiary lymphoid neogenesis and in situ antigen-driven clonal B cell selection. The autoantigen(s) driving in situ B cell selection in TII are not known. This study was undertaken to identify the dominant driving autoantigen(s).**

Methods. **Single CD38+ or Ki-67+ B cells were laser captured from 7 biopsy specimens that were diagnostic for LN. Eighteen clonally expanded immunoglobulin heavy- and light-chain variable region pairs were cloned and expressed as monoclonal antibodies. Seven more antibodies were cloned from flow-sorted CD38+ cells from an eighth biopsy specimen. Antigen characterization was performed using a combination of confocal microscopy, enzyme-linked immunosorbent assay, screening protoarrays, immunoprecipitation, and mass spectrometry. Serum IgG titers to the dominant antigen in 48 LN and 35 non-nephritic lupus samples were determined using purified antigen-coated arrays. Autoantigen expression on normal and LN kidney was localized by immunohistochemistry and immunofluorescence.**

Results. **Eleven of 25 antibodies reacted with cytoplasmic structures, 4 reacted with nuclei, and none reacted with double-stranded DNA. Vimentin was the only autoantigen identified by both mass spectrometry and protoarray. Ten of the 11 anticytoplasmic TII antibodies directly bound vimentin. Vimentin was highly expressed by tubulointerstitial inflammatory cells, and the TII antibodies tested preferentially bound inflamed tubulointerstitium. Finally, high titers of serum antivimentin antibodies were associated with severe TII ($P = 0.0001$).**

Conclusion. **Vimentin, an antigenic feature of inflammation, is a dominant autoantigen targeted in situ in LN TII. This adaptive autoimmune response likely feeds forward to worsen TII and renal damage.**

Systemic lupus erythematosus (SLE) is the archetypical systemic autoimmune disease, in which a break in both B and T cell tolerance enables pathogenic adaptive immunity to ubiquitous nuclear self antigens (1). In this model, antibodies and lymphocytes disseminate from secondary lymphoid organs to cause damage in end organs including the kidneys, lungs, skin, gastrointestinal tract, brain, and heart (2). Renal inflammation is a common, severe manifestation of SLE (3,4) that is often resistant to treatment with cytotoxic therapies (5). Up to 50% of SLE patients develop nephritis, which, in up to 50% of those affected, progresses to renal failure within 5 years (6,7).

Supported by the NIH (grant AR-55646 and Autoimmunity Centers of Excellence program grant AI-082724). Dr. Haddon is recipient of a Canadian Institutes for Health Research Fellowship.

[1]Andrew J. Kinloch, PhD, Kichul Ko, MD, Carole J. Henry Dunand, PhD, Scott Henderson, BS, Natalya Kaverina, MD, PhD, Marlene Salgado Ferrer, BS, Don Wolfgeher, BS, Vladimir Liarski, MD, Patrick C. Wilson, PhD, Marcus R. Clark, MD: University of Chicago, Chicago, Illinois; [2]Anthony Chang, MD: University of Chicago Medical Center, Chicago, Illinois; [3]Mark Maienschein-Cline, PhD: University of Illinois at Chicago; [4]Brad H. Rovin, MD: The Ohio State University, Columbus; [5]D. James Haddon, PhD, Paul J. Utz, MD: Stanford University, Stanford, California.

Dr. Rovin has received consulting fees, speaking fees, and/or honoraria from Biogen Idec, Bristol-Myers Squibb, Lilly, AstraZeneca, and Celtic Pharma (less than $10,000 each) and from GlaxoSmithKline (more than $10,000). Drs. Kinloch and Clark have submitted a patent application pertaining to the use of antivimentin antibodies in the diagnosis of tubulointerstitial nephritis.

Address correspondence to Marcus R. Clark, MD, Section of Rheumatology, Department of Medicine, Gwen Knapp Center for Lupus and Immunology Research, University of Chicago, JFK R310, 924 East 57th Street, Chicago, IL 60637. E-mail: mclark@medicine.bsd.uchicago.edu.

Submitted for publication March 21, 2014; accepted in revised form September 18, 2014.

The principal lesion within the kidney that is associated with systemic autoimmunity is glomerulonephritis (GN). GN is associated with serum anti–double-stranded DNA (anti-dsDNA) antibodies that often deposit in glomeruli (8,9). In animal models, some anti-dsDNA antibodies can induce GN (10,11).

In human lupus nephritis (LN), tubulointerstitial inflammation (TII) is also common. Severity of TII on renal biopsy, rather than severity of GN, predicts progression to renal failure (6,7,12). Furthermore, unlike GN, severe TII is associated with in situ adaptive immunity. Tertiary lymphoid organ–like structures, including T:B cell aggregates, plasmablast foci, and germinal centers (GCs), are common in severe TII (13,14). In situ antigen-driven selection of B cells occurs in each of these structures. Thus, human LN appears to arise from both systemic and in situ autoimmune responses, with the latter more closely associated with a poor prognosis (6,7,12).

The antigens driving in situ adaptive immunity in LN are not known. Therefore, in the present study we characterized a panel of in situ–selected IgGs from renal biopsy specimens. Vimentin, an antigen induced in TII, was the most commonly targeted autoantigen. Furthermore, high serum titers of antivimentin antibodies (AVAs) were restricted to patients with severe TII. These findings suggest that AVAs might be a useful biomarker of an in situ adaptive immune mechanism associated with severe TII.

MATERIALS AND METHODS

Patient samples. Patients at the University of Chicago and The Ohio State University who met the American College of Rheumatology 1982 revised criteria for SLE (15) were retrospectively selected. All patients provided informed consent, and the study was approved by the relevant institutional review boards.

Monoclonal antibody generation. Briefly, frozen biopsy specimens (13) were sectioned (7 μm), adhered to microscope slides, fixed in acetone (10 minutes, −20°C), washed with ice-cold phosphate buffered saline (PBS), and blocked with 10% donkey serum (Jackson ImmunoResearch). Sections were stained with anti-CD38 antibodies (2 μg/ml; Dako) or anti–Ki-67 antibodies (2 μg/ml; Thermo Scientific) conjugated with fluorescein isothiocyanate (FITC; Life Technologies) in PBS/5% donkey serum. Positively stained single cells were captured using an Arcturus Pixcell II and Capsure HS LCM caps (both from Molecular Devices) with an infrared laser (810 μm) spot diameter of 7.5 μm, 70 mW pulse power, 5 msec pulse duration, and 170 mW voltage (13). Caps were extracted as described previously (13).

One biopsy sample was digested for 30 minutes at 37°C in 5 ml digestion buffer (2 μg/ml collagenase B, 0.2 μg/ml DNase I, 1% bovine serum albumin [BSA], 25 m*M* $NaHCO_3$, 10 m*M* HEPES in Hanks' balanced salt solution), passed through a 200-μm nylon cell strainer, and resuspended in fluorescence-activated cell sorting (FACS) buffer. Single CD19+CD38+ cells were sorted into 96 well plates containing lysis buffer. Messenger RNA was reverse transcribed (16), and V_H (IgG) and V_L (κ and λ) regions were polymerase chain reaction–amplified and cloned into TOPO vectors (Life Technologies), sequenced, and analyzed (13,17). Paired V_H and V_L sequences were subcloned into their respective IgG1 heavy, λ, or κ expression vectors, and human IgG1 monoclonal antibodies (mAb) were produced (16).

Confocal microscopy. In initial experiments, antinuclear antibody (ANA) staining patterns of TII mAb were visualized using an indirect immunofluorescence kit (Inova diagnostics). For subsequent studies, HEp-2 cells were fixed in methanol (18) and incubated with mAb (50 μg/ml), followed by Alexa Fluor 488–conjugated goat anti-human IgG (2 μg/ml) and Hoechst 33342 (both from Life Technologies). Selected slides were sequentially stained with anti–vimentin V9 (2 μg/ml; Dako) or antigiantin (1 μg/ml; Abcam) followed by Alexa Fluor 568–conjugated donkey anti-mouse antibodies (2 μg/ml; Molecular Probes). Samples were imaged using a Leica SP5 II Sted-CW laser scanning confocal microscope.

Protein purification and identification. Cells were lysed on ice in radioimmunoprecipitation assay buffer (5×10^6 cells/0.5 ml). Clarified lysates were precleared with protein G–agarose (Pierce) and then incubated with mAb mixtures (200 μg total prebound to protein G–agarose) overnight at 4°C. Following washing in ice-cold immunoprecipitation wash buffer (25 m*M* Tris, 150 m*M* NaCl [pH 7.2]), immunoprecipitations were resolved by reducing sodium dodecyl sulfate–polyacrylamide gel electrophoresis (SDS-PAGE) (4–12% Bis-Tris; Life Technologies). Gels were stained with Instant Blue (Expedeon) and gel tranches (T1–4) excised. Tranches were reduced, alkylated, and trypsinized, for high-performance liquid chromatography–tandem mass spectrometry (MS/MS) (19). Scaffold (version 4.0.4; Proteome Software) was used to validate MS/MS-based peptide and protein identifications. Peptide identifications were accepted at >99.0% probability to achieve a false discovery rate of <1.0% (20), and protein identifications were accepted at >93.0% probability to achieve a false discovery rate of <1.0% (Protein Prophet) (21).

Protoarrays. Human protoarrays (Life Technologies) were blocked with PBS/2% BSA, rinsed with 0.05% PBS–Tween 20, and then incubated with 25 μg/ml mAb in PBS/2% BSA. Bound antibody was detected with Cy5-conjugated goat anti-human IgG (0.5 μg/ml; Jackson ImmunoResearch) and counterstained with rabbit anti-GST (Millipore) followed by Cy3-conjugated goat anti-rabbit IgG (0.5 μg/ml; Jackson ImmunoResearch). Antigen signals (mean fluorescence intensity [MFI]) were quantified using a GenePix 4000B microarray scanner and GenePix Pro 6.0 software (Molecular Devices).

Using raw values for the MFI of each probe spot for Cy5 (F635) and Cy3 (F532), and of the probe background for Cy5 (B635) and Cy3 (B532), initial probe intensities were computed as (F635/B635)/(F532/B532). Raw probe intensities were normalized to internal controls and linearly scaled to a median control probe intensity of 1.0. Each array was scanned at 2 photomultiplier tube (PMT) voltages, 500 and 600. At PMT 500, we assessed the ratio and the difference between

antibody and control intensities, i.e., R500 = A500/C500 and D500 = A500 − C500, respectively (A = antibody, C = control); the same was done for PMT 600. The overall probe reactivity was then computed as the harmonic mean, i.e., 4/([1/R500] + [1/R600] + [1/D500] + [1/D600]).

Vimentin microarrays. Bovine vimentin (100 μg/ml in 0.4*M* HCl; Sigma) was diluted 1:1 with printing buffer (ArrayIt) and spotted (20 features/block, 24 blocks/slide) onto SuperEpoxy glass slides using a SpotBot 3 microarrayer (ArrayIt). Slides were washed with 0.05% PBS–Tween 20 and then incubated in BlockIt blocking buffer (ArrayIt). Serum (1:50) or mAb (100 μg/ml) in reaction buffer (ArrayIt) was applied, followed by Cy3-conjugated goat anti-human IgG (0.5 μg/ml). Signals were quantified using a GenePix 4000B microarray scanner and GenePix Pro 6.0 software. The MFIs for the 20 vimentin features in each probed block were median averaged.

TII mAb staining of kidney tissue. Fresh frozen biopsy sections (3 μm were adhered to glass slides fixed in acetone (−20°C), washed in PBS, and permeabilized in PBS/0.5% Nonidet P40. Slides were blocked in PBS/10% donkey serum and probed with FITC-conjugated TII mAb (Pierce). Bound mAb was detected with rabbit anti-FITC antibodies (1 μg/ml; Life Technologies), followed by Alexa Fluor 488–conjugated goat anti-rabbit antibodies (0.5 μg/ml; Life Technologies). Cell nuclei were counterstained with Hoechst 33342.

RESULTS

Characterization of in situ–expressed immunoglobulins. Evidence of in situ antigen-driven B cell selection in LN includes the presence of intrarenal GCs, T:B cell aggregates, and plasmablast foci (13), all of which have been demonstrated histologically to contain Ki-67+ B cells and/or plasmablasts. To characterize the antigen(s) driving in situ B cell selection in each of these tertiary lymphoid-like structures, we identified a cohort of 8 lupus patients with TII found on diagnostic biopsy (see Supplementary Table 1, on the *Arthritis & Rheumatology* web site at http://onlinelibrary.wiley.com/doi/10.1002/art.38888/abstract). T:B cell aggregates and plasma cells were observed in 7 of the biopsy samples, and a GC in 1.

To identify in situ–selected B cell populations, 5 of the biopsy specimens with T:B cell aggregates and plasma cells (patients 1–5) were sectioned and stained for Ki-67. The specimen containing a GC (patient 6) and 1 specimen with T:B cell aggregates and plasma cells (patient 7) were stained for CD38. Positive cells were laser captured. From each capture, expressed IgG heavy chain or lambda or kappa variable (V_γ, V_λ, or V_κ) regions were amplified and subcloned into TA vectors (13). Multiple colonies from each transformation were sequenced. A particular variable chain sequence was considered valid if the same sequence was obtained from at least 2 separate colonies of a given transformation. A V_H and V_L pair was considered valid if the same immunoglobulin heavy chain rearrangement was obtained from at least 1 different captured area from 1 biopsy sample. Using this approach, 18 paired V_H and V_L regions were identified (Supplementary Table 2, http://onlinelibrary.wiley.com/doi/10.1002/art.38888/abstract).

For most patient samples, the above approach produced single V_H and V_L pairings. However, in 1 instance (patient 4), 2 heavy and 2 light chains persistently co-occurred. In this case, all 4 possible pairings were considered and expressed as respective mAb (Ki4-1 through Ki4-4). Additionally, 3 of the cloned heavy chains persistently co-occurred with 2 light chains, leading us to generate 2 different TII mAb for each respective heavy chain (patient 2, Ki2-1 and Ki2-2; patient 3, Ki3-1 and Ki3-2; patient 6, GC1 and GC1a).

Finally, 1 biopsy specimen was digested and single CD38+ cells were sorted by FACS (16). The variable regions were again subcloned into TA vectors and sequenced. Seven distinct V_H and V_L pairings were isolated.

A summary of the nucleotide and predicted amino acid sequences for individual V_H and V_L regions is provided in Supplementary Table 2. The V_H segments were different for each antibody chain, with the exception that both Ki5-1 and PB1 used V_H3-15, but with different D and J_H segments. Overall, the frequency of V_H segments was similar to V_H usage in the peripheral B cells of healthy subjects (22), including a bias for V_H3 (12 of 20) and V_H4 (7 of 20). The length of the V_H complementarity-determining region 3 and the V_L complementarity-determining region 3 varied from 7 to 23 amino acids and from 8 to 12 amino acids, respectively. All immunoglobulin heavy and light chains were somatically mutated (Supplementary Table 2), and a distribution of replacement and silent mutations consistent with antigen-driven selection (17) was evident in 13 of 20 V_H chains (Supplementary Table 3 on the *Arthritis & Rheumatology* web site at http://onlinelibrary.wiley.com/doi/10.1002/art.38888/abstract).

Frequent recognition of cytoplasmic antigens by antibodies from in situ–selected B cells. Paired V_H and V_L regions were subcloned and expressed as functional human IgG1 mAb. In total, 25 TII mAb were derived from 8 patients: 14 from Ki-67+ cells, 3 from CD38+ cells within a GC, 1 from CD38+ cells within a T:B cell aggregate, and 7 from a biopsy specimen sorted for CD38+ cells (Supplementary Tables 1 and 2).

All 25 TII mAb were assayed for nuclear reactivity by indirect immunofluorescence on HEp-2 cells (Figures 1A–C). Only 4 reacted preferentially with nuclear antigens, 3 of which exhibited speckled patterns and 1 a nucleolar pattern. In contrast, the control human IgG1 mAb, 3H9, which preferentially binds dsDNA, yielded a homogeneous nuclear staining pattern and reacted to a lesser extent with the cytoplasm.

Eleven antibodies, from 7 of the 8 patients, bound cytoplasmic antigens. Of these, 7 had preferential cytoskeletal reactivity, 2 displayed a diffuse homogeneous cytoplasmic pattern, and 2 had both cytoplasmic and nuclear binding. One mAb (PB7) colocalized with the Golgi apparatus protein giantin (23) (representative images available from the corresponding author upon request). Nine of 25 mAb demonstrated no detectable reactivity. These data suggest that TII in situ adaptive immune responses are more often targeted to cytoplasmic than to nuclear self antigens.

Infrequent binding of TII antibodies to nuclear antigens commonly associated with SLE. To confirm the absence of dsDNA reactivity, *Crithidia luciliae* were stained with each mAb. While mAb 3H9 exhibited strong reactivity with the kineticore, there was no detectable reactivity with the TII mAb. ELISAs for ANA, SSA, and Sm/RNP reactivity were subsequently performed. Interestingly, none of the 4 nuclear-reactive mAb (PB2, Ki1-2, Ki4-2, and Ki5-3) showed strong reactivity with any of these substrates. Ki4-2 did, however, have low reactivity with Sm/RNP. These findings suggest that the nuclear antigen specificities normally associated with SLE are not commonly selected in situ in lupus TII. Furthermore, none of the TII antibodies exhibited appreciable IgG rheumatoid factor activity. Representative images from the above-described experiments are available from the corresponding author upon request.

Vimentin is an autoantigen commonly targeted in situ. We next sought to identify the antigenic targets of antibodies with cytoplasmic and cytoskeletal reactivities (both collectively grouped as anti-cyto antibodies). We first interrogated protoarrays containing 9,400 human proteins, with a selected group of TII mAb (Figure 2). The measures of respective antigen reactivities were computed as harmonic mean ratios (see Materials and Methods). We validated the protoarrays with a transglutaminase 2 (TG2)–reactive human IgG1 mAb (4B06), cloned from a patient with celiac disease (24). The 2

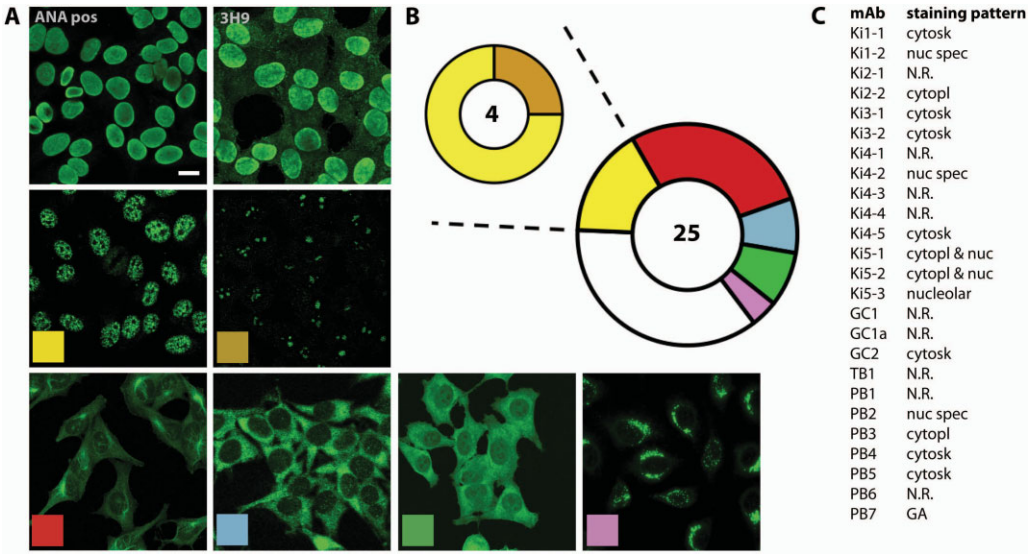

Figure 1. HEp-2 staining patterns obtained using tubulointerstitial inflammation (TII) monoclonal antibodies (mAb). **A,** Indirect immunofluorescence microscopy of HEp-2 cells following staining with TII mAb (25 μg/ml). Representative examples are shown. Positive controls include a known antinuclear antibody–positive (ANA pos) serum sample and the human IgG1 mAb 3H9, both of which exhibit preferential reactivity for DNA and a characteristic homogeneous nuclear staining pattern. The color key in each of the other 6 images represents the staining pattern being illustrated, as follows: yellow = nuclear speckled (nuc spec); brown = nucleolar; red = cytoskeletal (cytosk); blue = cytoplasmic (cytopl); green = cytoplasmic and nuclear; pink = Golgi apparatus (GA); white = no reactivity (N.R.). Bar = 10 μm. **B,** Pie charts summarizing the relative frequencies of HEp-2 staining patterns observed for TII mAb. The smaller chart is a subdivision of the mAb that preferentially reacted with nuclear antigens. Colors correspond to the color key described in **A**. **C,** Staining patterns of the respective TII mAb.

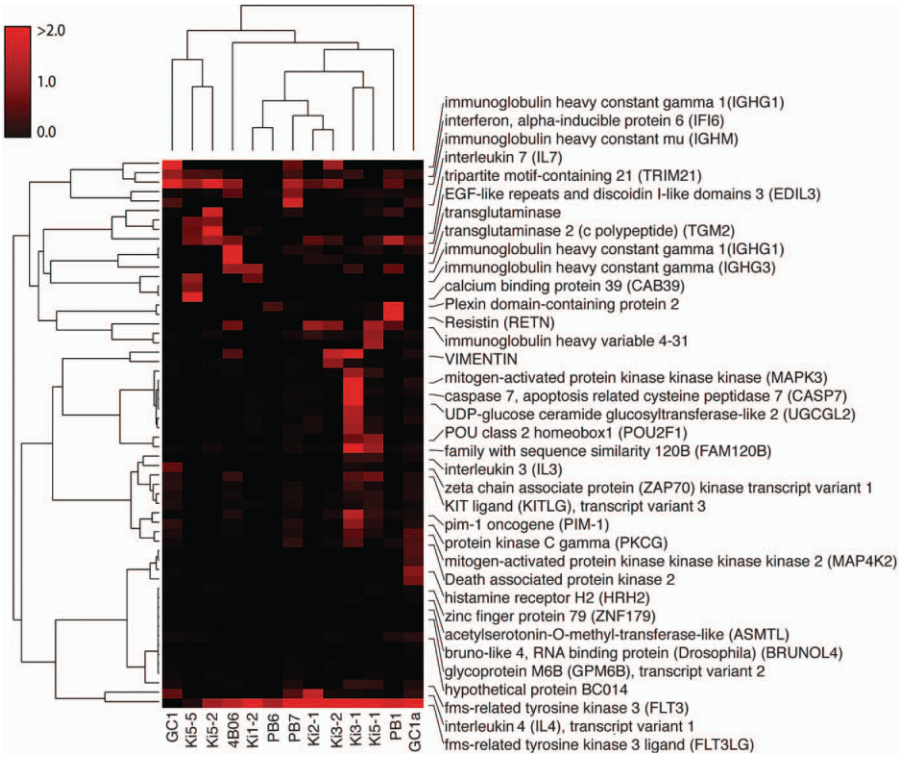

Figure 2. Immunoreactivities of tubulointerstitial inflammation monoclonal antibodies (mAb) with protoarrays. Antibodies with high reactivity in at least one array (defined as ≥2-fold higher than in 99% of control probes in the same array) were hierarchically clustered by antigen immunoreactivity. Protoarrays were validated using 4B06, a human IgG1 mAb that has known immunoreactivity with transglutaminase 2. The key at the top left indicates the magnitude of immunoreactivity (see Materials and Methods). EGF = epidermal growth factor.

TG2 antigens (IVGN:PM_2144 and BC003551) were the most highly reactive features, yielding values of 32.8 and 11.7, respectively.

The TII mAb used for protoarray probing provided at least one example of each staining pattern: anti-cyto (Ki5-2, Ki3-2, Ki3-1, Ki5-1), speckled nuclear (Ki1-2), Golgi apparatus (PB7), nucleolar (Ki5-3), and no appreciable HEp-2 reactivity (GC1, GC1a, PB6, Ki2-1, PB1). A subset of antigens was hierarchically clustered using a Pearson correlation distance measure and displayed in a heat map (Figure 2); the antigens selected were those with reactivity >2-fold the 99% value of the control probes. The most commonly reactive targets included Flt-3 ligand (FLT-3LG), IgG1 and IgM heavy chains, and epidermal growth factor (EGF)–like discoidin I–like domains 3. Essentially all of the antibodies bound FLT-3LG, and therefore this immunospecificity was likely spurious.

Most TII mAb, comparably to the TG2-specific mAb, displayed restricted polyreactivity with ≤8 proteins. In contrast, Ki3-1 displayed greater polyreactivity. Antigens targeted by at least 2 anti-cyto TII mAb included EGF-like discoidin I–like domains 3 and vimentin. In contrast, the nuclei-reactive mAb, Ki1-2, only bound weakly to a few protoarray antigens. A similar pattern of pauci-reactivity was observed with those TII mAb that did not react with HEp-2 cells.

We next used mass spectrometry to characterize the antigens targeted by the TII anti-cyto mAb (Figures 3A and B). HEp-2 cell lysates were immunoprecipitated with a mixture of anti-cyto mAb (Ki3-1, Ki3-2, Ki5-1, Ki5-2) or a mixture of 4 different anti-TG2 IgG1 mAb (4B06, 4A06, 4D03, 4E05) (24). Lysates were also immunoprecipitated with the antinucleolar mAb Ki5-3 (see Supplementary Table 4, on the *Arthritis & Rheumatology* web site at http://onlinelibrary.wiley.com/doi/10.1002/art.38888/abstract). Samples were resolved by reducing SDS-PAGE and stained with Coomassie blue (Figure 3A). A few unique bands were detected in the anti-cyto mAb lane, including one with a relative molecular weight of ~45 kd (T1). The T1 band, and a region corresponding to the same molecular weight from the

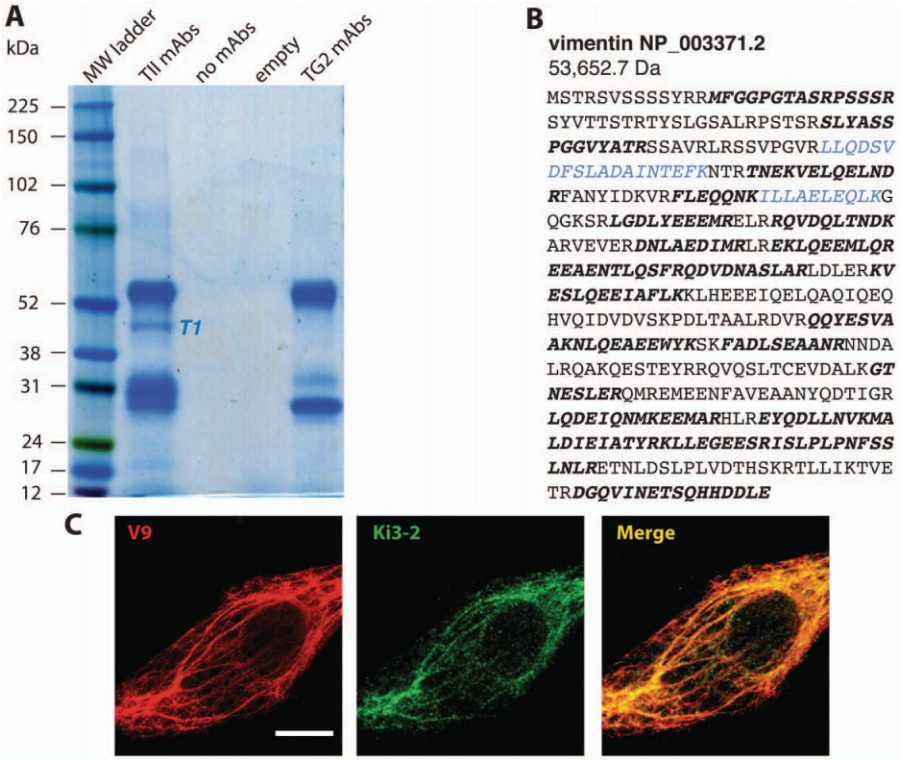

Figure 3. Identification of vimentin as a putative antigen targeted by tubulointerstitial inflammation (TII) monoclonal antibodies (mAb). **A,** Immunoprecipitations of HEp-2 cell lysates with either TII mAb (Ki3-1, Ki3-2, Ki5-1, and Ki5-2), no mAb, or transglutaminase 2 (TG2)–reactive mAb. Samples were resolved by reducing sodium dodecyl sulfate–polyacrylamide gel electrophoresis and stained with Coomassie blue. A unique TII mAb band (T1) was excised and analyzed by mass spectrometry. Among the proteins identified was vimentin. **B,** Vimentin as an antigen identified from peptides characterized from TII mAb immunoprecipitates of HEp-2 cell lysate. The vimentin (NP_003371.2) amino acid FASTA sequence in regions corresponding to peptides identified by mass spectrometry of T1 is shown in blue italics. Tranches cut from analogous immunoprecipitates (Supplementary Tables 4 and 5, on the *Arthritis & Rheumatology* web site at http://onlinelibrary.wiley.com/doi/10.1002/art.38888/abstract), generated with other TII mAb, yielded additional vimentin peptides (boldface italics). **C,** Confocal microscopy of HEp-2 cells, demonstrating costaining of TII mAb Ki3-2 with antivimentin mAb V9. Bar = 10 μm.

Ki5-3 immunoprecipitation (T2), were excised for mass spectrometry. From the T1 band, proteins inferred from peptide spectra were cytokeratins 1, 2, 7, and 9, actin, fructose biphosphate aldolase A, and vimentin (see Supplementary Table 5, on the *Arthritis & Rheumatology* web site at http://onlinelibrary.wiley.com/doi/10.1002/art.38888/abstract). Among the above-mentioned proteins identified from T1, the cytokeratins were also observed in T2. Cross-referencing of the T1 proteins identified by mass spectrometry with those on the protoarray heatmap (Figure 2) revealed that only vimentin was common. The 2 vimentin peptides identified by mass spectrometry (Figure 3B and Supplementary Tables 4 and 5) represented 29 of the 466 amino acids (6%) in the full-length translated protein.

Additional immunoprecipitations were performed with a different mixture of cytoskeleton-staining TII mAb (GC2, Ki4-5, PB4, and PB5) using lysates of HEp-2 or primary renal proximal epithelial cells. As full-length vimentin has a relative molecular weight of 54 kd, gel tranches covering 50–55 kd were excised (Supplementary Table 5) for mass spectrometry. Vimentin peptides were once again identified in both samples. The lower molecular weight forms of vimentin detected in T1 likely represent proteolytic fragments (25,26). In total, 27 different vimentin peptides covering 259 amino acids (56% of the full length protein) (Figure 3B) were identified from T1, T3, and T4 (Supplementary Table 5). To confirm that vimentin was targeted by TII anti-cyto mAb, HEp-2 cells were costained with the TII mAb Ki3-2 and the murine antivimentin mAb V9 (Figure 3C), revealing extensive colocalization.

To determine whether vimentin was a frequent target of antibodies produced in situ during TII, all 10

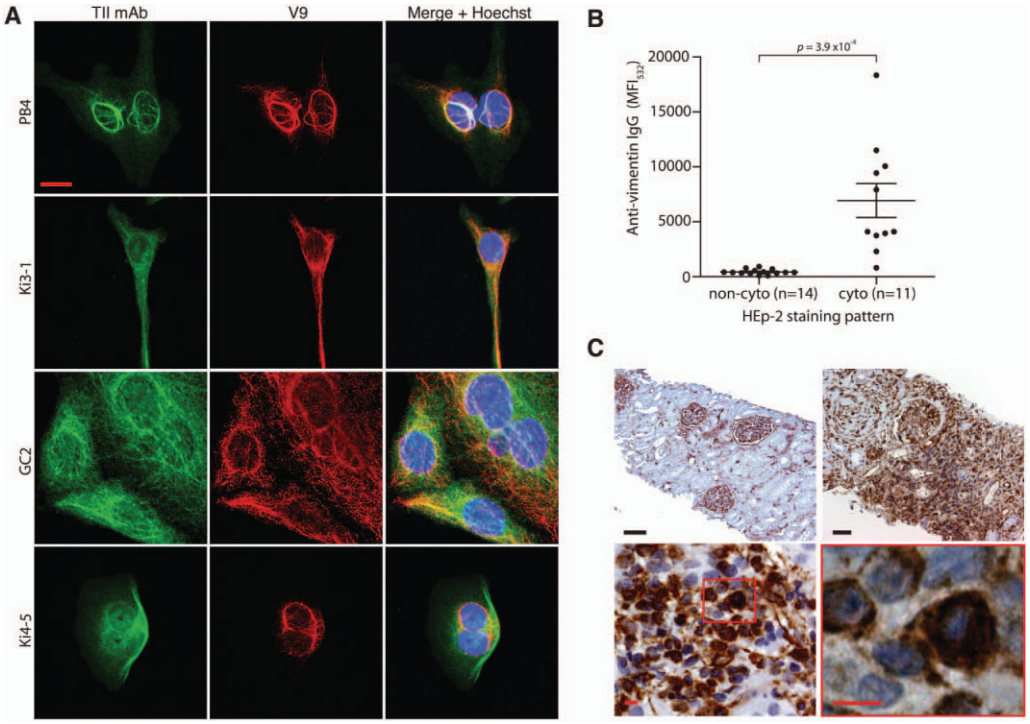

Figure 4. Frequent targeting of vimentin by tubulointerstitial inflammation (TII) monoclonal antibodies (mAb). **A,** HEp-2 cells costained with TII mAb (green), antivimentin (V9) (red), and Hoechst (blue). Examples of 4 different patterns of colocalization are shown. Examples of staining with TII mAb with cytoplasmic reactivity are available from the corresponding author upon request. **B,** Results of probing of vimentin protein arrays with the TII mAb grouped by presence or absence of cytoplasmic (cyto) HEp-2 immunoreactivity, detected with anti-human IgG_{532}. Each data point represents the reactivity of an individual TII mAb (raw mean fluorescence intensity [MFI]); horizontal lines and error bars show the median and interquartile range. *P* value was determined by Mann-Whitney 2-tailed test. **C,** Immunohistochemical staining of normal kidney tissue (top left) and TII kidney tissue (other panels) with V9 antibody. Boxed area in the bottom left panel is shown at higher magnification in the bottom right panel. Black bars and red bars = 100 μm and 10 μm, respectively.

remaining anti-cyto TII mAb were assayed by confocal microscopy. All 10 had some overlap with V9 staining, with PB4, Ki3-1, GC2, PB3, PB5, and Ki1-1 showing extensive and specific overlap (Figure 4A). Polyreactivity was observed with TII mAb Ki2-2, Ki5-1, and Ki5-2 (images available from the corresponding author upon request), while Ki4-5 (Figure 4A) exhibited preferential staining of cytoskeletal filaments, some of which did not react with V9. As these colocalizations could represent binding to antigens closely neighboring vimentin, direct vimentin immunoreactivity was confirmed using purified bovine vimentin–coated SuperEpoxy glass slides (Figure 4B). Ten of 11 anti-cyto TII mAb displayed vimentin immunoreactivity greater than that observed with any of the non-cyto TII mAb ($P = 3.9 \times 10^{-4}$) (Figure 4B).

Up-regulation of vimentin in inflamed tubulointerstitium. To investigate why vimentin was so commonly targeted in situ, we examined the distribution of vimentin expression in normal and LN renal biopsy samples by immunohistochemistry (Figure 4C). Consistent with previous reports (25,27), in normal kidney vimentin was expressed primarily in glomeruli, arterioles, and interstitial fibroblasts, but not in epithelial cells. In contrast, the distribution and intensity of vimentin expression in TII specimens was radically different, with vimentin being abundant throughout the tubulointerstitium. Much of this increased vimentin expression localized to the mononuclear cells infiltrating the tubulointerstitium.

High expression of vimentin by infiltrating mononuclear cells suggested that in situ humoral immunity is directed against molecules associated with inflammation. Therefore, we directly examined whether TII mAb also preferentially bound inflamed tubulointerstitium (Figure 5). Two TII mAb, Ki3-1 and PB4, both with vimentin immunoreactivity, were directly labeled with FITC and used to stain sections from normal kidney and LN kidney with severe TII. Samples were then incubated

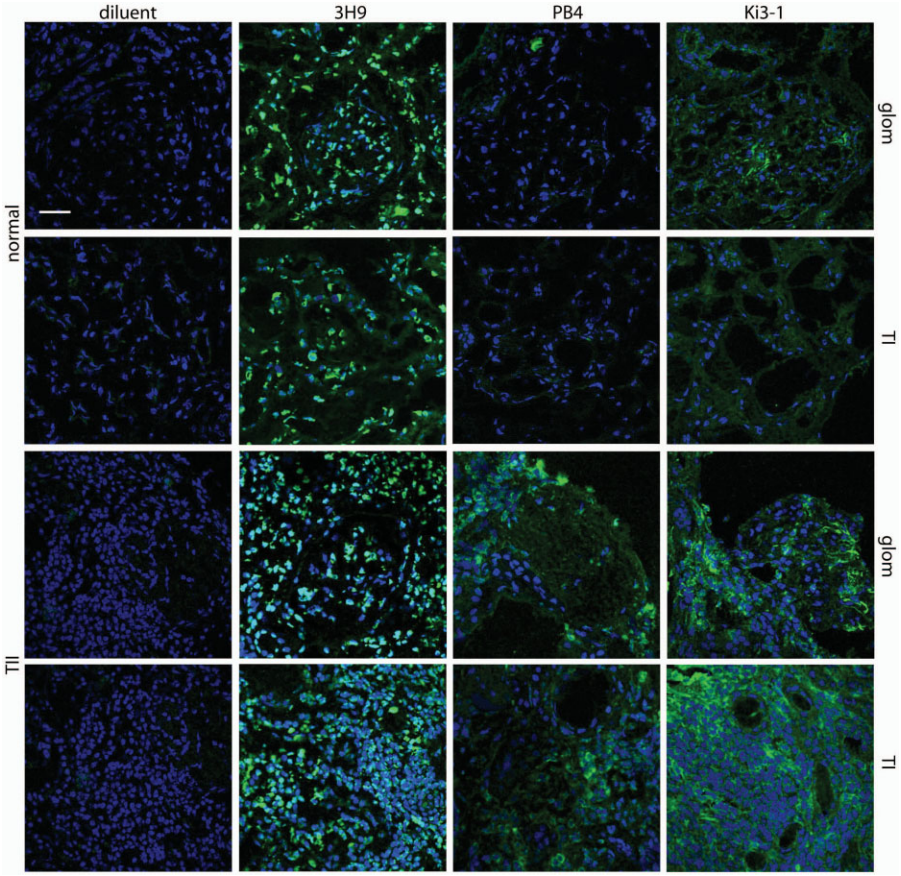

Figure 5. Enhanced binding of tubulointerstitial inflammation (TII) monoclonal antibodies (mAb) to inflamed renal tubulointerstitium. The indicated TII mAb were used to stain normal renal and TII samples, with mAb 3H9 and diluent used as positive and negative controls, respectively. Tissue was counterstained with Hoechst for nuclei (blue). Representative patterns of tubulointerstitial and glomerular (glom) binding are shown. Bar = 100 μm.

with rabbit anti-FITC antibodies followed by Alexa Fluor 488–conjugated goat anti-rabbit antibodies (images available from the corresponding author upon request). As expected, no discernible immunoreactivity was detected in the absence of primary antibody (Figure 5). In contrast, staining with 3H9 yielded a predictable nuclear pattern. In normal kidney, Ki3-1 had some immunoreactivity with glomeruli and minimal immunoreactivity with the tubulointerstitium. PB4 demonstrated little immunoreactivity with normal renal tissue. In contrast, both antibodies bound inflamed tubulointerstitium, and Ki3-1 also bound inflamed glomeruli. These results are consistent with a model in which in situ immunity targets inflammation.

Association of serum AVAs with severe TII. As vimentin is frequently targeted by the in situ humoral immune response, we predicted that serum AVA titers would reflect TII severity. To investigate this, AVA titers in serum samples from SLE patients with LN (n = 48) or with no history of renal disease (n = 35) were assayed as described above (Figures 6A and B). High-titer AVAs (>180 AU) were found almost exclusively in patients with renal disease, and the average AVA titer was higher in this group than in the group without renal disease ($P = 0.01$). The 1 SLE patient without renal involvement who had a relatively high AVA titer had very active extrarenal disease, with severe discoid lupus, arthritis, vasculitis, decreased serum complement levels, and increased anti-dsDNA antibody titers. Within the group with renal involvement, high-titer AVAs strongly correlated with severe (grade 3) TII ($P < 0.0001$), with the 5 highest AVA titers detected among patients with grade 3 TII. Only 1 of 10 patients with severe TII had low-titer AVAs. These data suggest that high-titer AVAs might be a useful biomarker of severe TII.

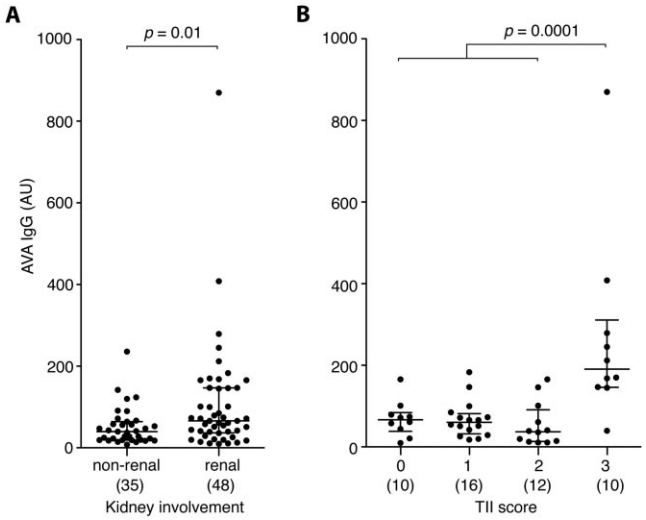

Figure 6. Association of nephritis with antivimentin IgG levels in the serum of patients with systemic lupus erythematosus. Individual serum samples were used to probe vimentin arrays for IgG reactivity. **A,** Patients were first grouped according to whether they did or did not have a history of nephritis. **B,** Patients with nephritis were further grouped according to the degree of tubulointerstitial inflammation (TII) (0 = none, 1 = mild, 2 = moderate, 3 = severe). Titers were extrapolated using a serially diluted sample from a patient with TII and high-titer antivimentin antibody (AVA). The number of patients in each group is shown in parentheses. Among patients with renal involvement, serum samples were obtained a median of 1.36 years after biopsy (interquartile range 0.08–3.14 years), and the mean ± SD age at the time serum samples were obtained was 33.1 ± 9.7 years. Among patients without renal involvement, the mean ± SD age at the time serum samples were obtained was 41.6 ± 10.5 years ($P < 0.01$ versus those with renal involvement). Each data point represents an individual patient; bars show the median and interquartile range. *P* values were determined by Mann-Whitney 2-tailed test.

DISCUSSION

In many previous studies, autoantibody specificities in serum were identified first, and subsequently were correlated with disease manifestations (2,28). In the present study, in contrast, we started with the affected end organ, providing immediate pathologic context. The relevance of the characterized in situ–derived antivimentin mAb to TII was supported by the correlation between high serum AVA titers and severe TII. Our results suggest that tissue-focused studies can identify clinically important biomarkers, and potentially pathogenic mechanisms, that are not immediately apparent from studies of peripheral blood.

In lupus patients with TII, in situ humoral immunity appeared to be antigenically restricted and primarily focused on cytoplasmic antigens—notably, vimentin. Vimentin was expressed by infiltrating inflammatory cells, and the TII mAb that were tested preferentially reacted with the inflamed tubulointerstitium. We postulate that by targeting inflammation the adaptive immune response, and the attendant deposition of antibodies and complement, feed forward to amplify local inflammation, tissue destruction, and renal scarring (29).

Of the other serologic specificities associated with SLE, only anti-dsDNA antibody titers provide a similar correlation with disease activity (30,31). This is best defined for GN, in which high-titer dsDNA antibodies predict renal flare in some patients (2) and anti-dsDNA antibodies deposited in inflamed glomeruli can be detected (9,32). While dsDNA antibody titers provide a measure of systemic autoimmunity, we suggest that AVA titers provide complementary measures of organ-intrinsic mechanisms of autoimmunity.

Most of the identified antigens targeted by the in situ humoral immune response were cytosolic proteins, the immune response to which usually requires T cell help (33). Indeed, follicular helper T cells are common in LN biopsy specimens that manifest severe TII, where they are in apparent cognate pairs with B cells (34). Therefore, the inflamed tubulointerstitium appears sufficient to propagate cytosolic antigen–targeted humoral immunity. In contrast, inflamed glomeruli lack infiltrating B and follicular helper T cells. B cell–expressed Toll-like receptors might therefore be less important in situ than they are in systemic immune responses measured in the periphery (and propagated in secondary lymphoid organs), where these receptors play a role in responses to dsDNA- and RNP-containing complexes (35,36).

Some characteristics of vimentin might enhance its antigenicity in situ. Vimentin is a highly basic molecule that is secreted by activated macrophages (26). Therefore, in inflammation, vimentin is abundant and available. Furthermore, vimentin can bind and activate dectin 1 (37), a C-type lectin receptor expressed on cells including macrophages, dendritic cells, and B cells. Vimentin might therefore locally prime antigen-presenting cells. Finally, vimentin can be posttranslationally modified, which, in rheumatoid arthritis, provides neoepitopes and increases antigenicity (38). It remains to be determined if posttranslational modifications enhance in situ immunity to vimentin in LN TII, or whether particular HLA molecules preferentially present vimentin-derived peptides. Mapping of dominant vimentin epitopes should provide insights into these questions.

Most AVAs we investigated exhibited polyreactivity. This could reflect a less efficient selection on

multiple abundant antigens in the inflamed kidney, in comparison to a predictably stringent selection in GCs, in which antigen is limited and presented in competitive contexts that favor higher affinity and restricted polyreactivity (39). Alternatively, the heightened polyreactivity/polyspecificity may be due to more than one antigen driving selection, reflecting polyselection.

Interestingly, anticytoplasmic antibodies are a common feature of the normal newly emigrated and mature naive B cell repertoires (40). Furthermore, in SLE, anticytoplasmic antibodies are even more frequent in these pools, with at least one-third of mature naive B cells having some cytoplasmic reactivity (41). The high prevalence of B cells expressing anticytoplasmic antibodies may help explain the low titers of AVAs observed in most SLE patients. Presumably, the TII AVAs that we characterized arose from one or more of the above B cell populations expressing anticytoplasmic antibodies. Alternatively, it is possible that the AVAs were selected from non-autoreactive or antinuclear antigen–specific B cell precursor populations.

High-titer AVAs (>225 arbitrary units [AU]) were invariably associated with high disease activity, usually severe TII. Among the 6 highest AVA titers, 5 occurred in patients with severe TII, with all 4 of the very highest titers associated with this manifestation. The only non-nephritic patient with high-titer AVAs (236 AU) had severe extrarenal disease. Intermediate AVA titers (150–220 AU) were preferentially found in patients with nephritis. Therefore, different titers of AVAs might reflect different levels of disease activity and disease manifestations.

Anticytoplasmic antibodies and AVAs have been observed in a variety of autoimmune diseases (42–45) and in transplant rejection. Interestingly, in cardiac allograft recipients, IgM AVAs are predictive of allograft vasculopathy (46) and rejection (47). Furthermore, AVAs have been observed in renal transplant rejection (48,49). In mice, immunization with vimentin accelerates cardiac allograft rejection (50), providing evidence that antivimentin immune responses can be pathogenic. These results, taken together with our findings reported herein, suggest that AVAs represent a common adaptive immune response in chronic organ inflammation, which perpetuates disease.

Because of the difficulties inherent in isolating in situ–selected B cells, our study was restricted to a small number of biopsy specimens and mAb. Sampling single cells by laser capture is imprecise, and it is likely that a few V_H and V_L pairings were spurious. Indeed, in some cases a single V_H could not be paired with a single V_L. Furthermore, closed needle biopsy provides a limited sampling of the entire lesion. Despite these limitations, our study revealed consistent themes: antibodies from 7 of 8 patients were immunoreactive with cytoplasmic antigens, and antibodies from 6 of 8 patients had vimentin immunoreactivity. Furthermore, these prevalences correlated with the frequency of high serum AVA titers in patients with severe TII. Therefore, our sample size and approach appeared sufficient to capture common features of the TII in situ adaptive immune response.

This study demonstrates that high AVA titers identify SLE patients with severe TII, a population at substantial risk for progression to renal failure (6,7,12). Whether AVAs are directly pathogenic, or if they can be used as a biomarker, requires additional study. Also, it is not known if high AVA titers identify patients who will be responders to targeted therapies. Regardless, knowing where and when AVAs arise in lupus will provide a strong context for interpreting future clinical and mechanistic studies.

ACKNOWLEDGMENTS

We would like to thank Christine Labno and Margaret Veselits for technical assistance with confocal microscopy, Justin Jarrel for technical assistance with antigen microarrays, and Keith Hamel and Sophiya Karki for critical reading of the manuscript.

AUTHOR CONTRIBUTIONS

All authors were involved in drafting the article or revising it critically for important intellectual content, and all authors approved the final version to be published. Dr. Clark had full access to all of the data in the study and takes responsibility for the integrity of the data and the accuracy of the data analysis.

Study conception and design. Kinloch, Haddon, Clark.

Acquisition of data. Kinloch, Chang, Henry Dunand, Henderson, Kaverina, Rovin, Salgado Ferrer, Wolfgeher, Liarski, Wilson.

Analysis and interpretation of data. Kinloch, Ko, Henderson, Maienschein-Cline, Wolfgeher, Liarski, Haddon, Utz, Clark.

REFERENCES

1. Liu Z, Davidson A. Taming lupus—a new understanding of pathogenesis is leading to clinical advances. Nat Med 2012;18: 871–82.
2. Lahita RG, Tsokos G, Buyon JP, Koike T, editors. Systemic lupus erythematosus. 5th ed. San Diego: Elsevier Academic Press; 2010.
3. Mok C, Tang SS. Incidence and predictors of renal disease in Chinese patients with systemic lupus erythematosus. Am J Med 2004;17:791–5.
4. Cervera R, Khamashta MA, Font J, Sebastiani GD, Gil A, Lavilla P, et al, European Working Party on Systemic Lupus Erythematosus. Morbidity and mortality in systemic lupus erythematosus during a 10-year period: a comparison of early and late manifes-

tations in a cohort of 1,000 patients. Medicine (Baltimore) 2003; 82:299–308.
5. Ginzler E, Dooley MA, Aranow C, Kim MY, Buyon J, Merrill JT, et al. Mycophenolate mofetil or intravenous cyclophosphamide for lupus nephritis. N Engl J Med 2005;353:2219–28.
6. Esdaile JM, Levinton C, Federgreen W, Hayslett JP, Kashgarian M. The clinical and renal biopsy predictors of long-term outcome in lupus nephritis: a study of 87 patients and review of the literature. Q J Med 1989;72:779–833.
7. Hsieh C, Chang A, Brandt D, Guttikonda R, Utset TO, Clark MR. Predicting outcomes of lupus nephritis with tubulointerstitial inflammation and scarring. Arthritis Care Res (Hoboken) 2011; 63:865–74.
8. Ebling F, Hahn BH. Restricted subpopulations of DNA antibodies in kidneys of mice with systemic lupus: comparison of antibodies in serum and renal eluates. Arthritis Rheum 1980;23:392–403.
9. Winfield JB, Faiferman I, Koffler D. Avidity of anti-DNA antibodies in serum and IgG glomerular eluates from patients with systemic lupus erythematosus: association of high avidity antinative DNA antibody with glomerulonephritis. J Clin Invest 1977;59:90–6.
10. Ehrenstein MR, Katz DR, Griffiths MH, Papadaki L, Winkler TH, Kalden JR, et al. Human IgG anti-DNA antibodies deposit in kidneys and induce proteinuria in SCID mice. Kidney Int 1995;48: 705–11.
11. Madaio MP, Carlson J, Cataldo J, Ucci A, Migliorini P, Pankewycz O. Murine monoclonal anti-DNA antibodies bind directly to glomerular antigens and form immune deposits. J Immunol 1987; 138:2883–9.
12. Yu F, Wu LH, Tan Y, Li LH, Wang CL, Wang CL, et al. Tubulointerstitial lesions of patients with lupus nephritis classified by the 2003 International Society of Nephrology and Renal Pathology Society system. Kidney Int 2010;77:820–9.
13. Chang A, Henderson SG, Brandt D, Liu N, Guttikonda R, Hsieh C, et al. In situ B cell-mediated immune responses and tubulointerstitial inflammation in human lupus nephritis. J Immunol 2011;186:1849–60.
14. Davidson A, Aranow C. Lupus nephritis: lessons from murine models. Nat Rev Immunol 2010;6:13–20.
15. Tan EM, Cohen AS, Fries JF, Masi AT, McShane DJ, Rothfield NF, et al. The 1982 revised criteria for the classification of systemic lupus erythematosus. Arthritis Rheum 1982;25:1271–7.
16. Smith K, Garman L, Wrammert J, Zheng NY, Capra JD, Ahmed R, et al. Rapid generation of fully human monoclonal antibodies specific to a vaccinating antigen. Nat Protoc 2009;4:372–84.
17. Lossos IS, Tibshirani R, Narasimhan B, Levy R. The inference of antigen selection on Ig genes. J Immunol 2000;165:5122–6.
18. O'Neill SK, Veselits ML, Zhang M, Labno C, Cao Y, Finnegan A, et al. Endocytic sequestration of the B cell antigen receptor and Toll-like receptor 9 in anergic B cells. Proc Nat Acad Sci U S A 2009;106:6262–7.
19. Truman AW, Kristjansdottir K, Wolfgeher D, Hasin N, Polier S, Zhang H, et al. CDK-dependent Hsp70 phosphorylation controls G1 cyclin abundance and cell-cycle progression. Cell 2012;151: 1308–18.
20. Keller A, Nesvizhskii AI, Kolker E, Aebersold R. Empirical statistical model to estimate the accuracy of peptide identifications made by MS/MS and database search. Anal Chem 2002;74: 5382–92.
21. Nesvizhskii AI, Keller A, Kolker E, Aebersold R. A statistical model for identifying proteins by tandem mass spectrometry. Anal Chem 2003;75:4646–58.
22. Brezinschek HP, Brezinschek RI, Lipsky PE. Analysis of the heavy chain repertoire of human peripheral B cells using single-cell polymerase chain reaction. J Immunol 1995;155:190–202.
23. Nozawa K, Fritzler MJ, von Muhlen CA, Chan EK. Giantin is the major Golgi autoantigen in human anti-Golgi complex sera. Arthritis Res Ther 2004;6:R95–102.
24. Di Niro R, Mesin L, Zheng NY, Stamnaes J, Morrissey M, Lee JH, et al. High abundance of plasma cells secreting transglutaminase 2-specific IgA autoantibodies with limited somatic hypermutation in celia disease interstinal lesions. Nat Med 2012;18:441–51.
25. Buchmaier BS, Bibi A, Muller GA, Dihazi GH, Eltoweissy M, Kruegel J, et al. Renal cells express different forms of vimentin: the independent expression alteration of these forms is important in cell resistance to osmotic stress and apoptosis. PLoS One 2013;8:e68301.
26. Mor-Vaknin N, Punturieri A, Sitwala K, Markovitz DM. Vimentin is secreted by activated macrophages. Nat Cell Biol 2003;5:59–63.
27. De Matos AC, Camara NO, Tonato EJ, de Souza Durao M Jr, Franco MF, Moura LA, et al. Vimentin expression and myofibroblast infiltration are early markers of renal dysfunction in kidney transplantation: an early stage of chronic allograft dysfunction? Transplant Proc 2010;42:3482–8.
28. Tan EM, Kunkel HG. Characteristics of a soluble nuclear antigen precipitation with sera of patients with systemic lupus erythematosus. J Immunol 1966;96:464–71.
29. Liu L, Kou P, Zeng Q, Pei G, Li Y, Liang H, et al. CD4+ T lymphocytes, especially Th2 cells, contribute to the progress of renal fibrosis. Am J Nephrol 2012;36:386–96.
30. Ter Borg EJ, Horst G, Hummel EJ, Limburg PL, Kallenberg CG. Measurement of increases in anti–double-stranded DNA antibody levels as a predictor of disease exacerbation in systemic lupus erythematosus. Arthritis Rheum 1990;33:634–43.
31. Bootsma H, Spronk PE, Ter Borg EJ, Hummel EJ, de Boer G, Limubrg PC, et al. The predictive value of fluctuations in IgM and IgG class anti-dsDNA antibodies for relapses in systemic lupus erythematosus: a prospective long-term observation. Ann Rheum Dis 1997;56:661–6.
32. Kalaaji M, Fenton KA, Mortensen ES, Olsen R, Sturfelt G, Alm P, et al. Glomerular apoptotic nucleosomes are central target structures for nephritogenic antibodies in human SLE nephritis. Kidney Int 2007;71:664–72.
33. Crotty S. Follicular helper CD4 T cells (T_{FH}). Annu Rev Immunol 2011;29:621–63.
34. Liarski V, Kaverina N, Chang A, Brandt D, Carlesso G, Utset TO, et al. Quantitative cell distance mapping in human nephritis reveals organization of in situ adaptive immune responses. Sci Transl Med. In press.
35. Shlomchik MJ. Sites and stages of autoreactive B cell activation and regulation. Immunity 2008;28:18–28.
36. Christensen SR, Shupe J, Nickerson K, Kashgarian M, Flavell RA, Shlomchik MJ. Toll-like receptor 7 and TLR9 dictate autoantibody specificity and have opposing inflammatory and regulatory roles in a murine model of lupus. Immunity 2006;25:417–28.
37. Thiagarajan PS, Yakubenko VP, Elsori DH, Yadav SP, Willard B, Tan CD, et al. Vimentin is an endogenous ligand for the pattern recognition receptor Dectin-1. Cardiovasc Res 2013;99:494–504.
38. Bang H, Egerer K, Gauliard A, Luthke K, Rudolph PE, Fredenhagen G, et al. Mutation and citrullination modifies vimentin to a novel autoantigen for rheumatoid arthritis. Arthritis Rheum 2007; 56:2503–11.
39. Shlomchik MJ, Weisel F. Germinal center selection and the development of memory B and plasma cells. Immunol Rev 2012;247:52–63.
40. Wardemann H, Yurasov S, Schaefer A, Young JW, Meffre E, Nussenzweig MC. Predominant autoantibody production by early human B cell precursors. Science 2003;301:1374–7.
41. Yurasov S, Wardemann H, Hammersen J, Tsuiji M, Meffre E, Pascual V, et al. Defective B cell tolerance checkpoints in systemic lupus erythematosus. J Exp Med 2005;201:703–11.

42. Ooka S, Nakano H, Matsuda T, Okamoto K, Suematsu N, Korokawa MS, et al. Proteomic surveillance of autoantigens in patients with Behçet's disease by a proteomic approach. Microbiol Immunol 2010;54:354–61.
43. Alcover A, Ramierez-Lafita F, Hernandez C, Nieto A, Avlia J. Antibodies to vimentin intermediate filaments in sera from patients with SLE and RA: quantitation by solid phase radioimmunoassay. J Rheumatol 1985;12:233–6.
44. Clemente MG, Musu MP, Frau F, Brusco G, Sole G, Corazza GR, et al. Immune reaction against the cytoskeleton in coeliac disease. Gut 2000;47:520–6.
45. Senecal JL, Oliver JM, Rothfeld N. Anticytoskeletal autoantibodies in connective tissue diseases. Arthritis Rheum 1985;28: 889–98.
46. Jurcevic S, Ainsworth ME, Pomerance A, Smith JD, Robinson DR, Dunn MJ, et al. Antivimentin antibodies are an independent predictor of transplant-associated coronary artery disease after cardiac transplantation. Transplantation 2001;71:886–92.
47. Nath DS, Ilias BG, Tiriveedhi V, Alur C, Phelan D, Eward GA, et al. Characterization of immune responses to cardiac self-antigens myosin and vimentin in human cardiac allograft recipients with antibody-mediated rejection and cardiac allograft vasculopathy. J Heart Lung Transplant 2010;29:1277–85.
48. Carter V, Howell WM. Vimentin antibody production in transplant patients and immunodulatory effects of vimentin in vitro. Hum Immunol 2013;4:1463–9.
49. Carter V, Shenton BK, Jaques B, Turner D, Talbot D, Gupta A, et al. Vimentin antibodies: a non-HLA antibody potential risk factor in renal tranplantation. Transplant Proc 2005;37:654–7.
50. Mahesh B, Leong JS, McCormak A, Sarathchandra P, Holder A, Rose ML. Autoantibodies to vimentin cause accelerated rejection of cardiac allografts. Am J Pathol 2007;170:1415–27.